Understanding the factors affecting the activation of alkane by Cp′Rh(CO)$_2$ (Cp′ = Cp or Cp*)

Michael W. George[a,1], Michael B. Hall[b,1], Omar S. Jina[a], Peter Portius[a,2], Xue-Zhong Sun[a], Michael Towrie[c], Hong Wu[b], Xinzheng Yang[b], and Snežana D. Zarić[d]

[a]School of Chemistry, University of Nottingham, University Park NG7 2RD, United Kingdom; [b]Department of Chemistry, Texas A&M University, College Station, TX 77843-3255; [c]Central Laser Facility, Science and Technology Facilities Council, Rutherford Appleton Laboratory, Harwell Science and Innovation Campus, Didcot OX11 0QX, United Kingdom; and [d]Department of Chemistry, University of Belgrade, Studentski Trg 16, P.O. Box 158, 11001 Belgrade, Serbia

Edited by Robert G. Bergman, University of California, Berkeley, CA, and approved August 21, 2010 (received for review February 26, 2010)

Fast time-resolved infrared spectroscopic measurements have allowed precise determination of the rates of activation of alkanes by Cp′Rh(CO) (Cp′ = η^5-C_5H_5 or η^5-C_5Me_5). We have monitored the kinetics of C—H activation in solution at room temperature and determined how the change in rate of oxidative cleavage varies from methane to decane. The lifetime of CpRh(CO)(alkane) shows a nearly linear behavior with respect to the length of the alkane chain, whereas the related Cp*Rh(CO)(alkane) has clear oscillatory behavior upon changing the alkane. Coupled cluster and density functional theory calculations on these complexes, transition states, and intermediates provide the insight into the mechanism and barriers in order to develop a kinetic simulation of the experimental results. The observed behavior is a subtle interplay between the rates of activation and migration. Unexpectedly, the calculations predict that the most rapid process in these Cp′Rh(CO)(alkane) systems is the 1,3-migration along the alkane chain. The linear behavior in the observed lifetime of CpRh(CO)(alkane) results from a mechanism in which the next most rapid process is the activation of primary C—H bonds (—CH_3 groups), while the third key step in this system is 1,2-migration with a slightly slower rate. The oscillatory behavior in the lifetime of Cp*Rh(CO)(alkane) with respect to the alkane's chain length follows from subtle interplay between more rapid migrations and less rapid primary C—H activation, with respect to CpRh(CO)(alkane), especially when the CH_3 group is near a *gauche* turn. This interplay results in the activation being controlled by the percentage of alkane conformers.

organometallic | photochemistry | computation | transition metal | sigma complex

Alkanes are generally unreactive molecules and the lack of ability to utilize such feedstock has thwarted the widespread use of methane, the main component of natural gas, as a feedstock to produce synthetically useful compounds even though this inexpensive source is widely available (1). The facile activation of methane is considered a "holy grail" for chemists (2). The use of transition metals in order to provide a way to activate carbon–hydrogen (C—H) bonds in hydrocarbons offers the potential to address this problem, and useful processes have been developed including alkane dehydrogenation, arene borylation, and alkane metathesis.

The early reports of alkane activation involved an initial photodissociation of a ligand, from a five-coordinate cyclopentadienyl rhodium(I) or iridium(I) complex to form a coordinatively unsaturated intermediate (3, 4). This reactive species subsequently attacks and oxidatively adds a C—H bond to form the alkyl hydride product. There has been considerable research effort directed toward understanding this key reaction in order to allow the full exploitation of the C—H activation process. The photochemistry of Cp′Rh(CO)$_2$ [Cp′ = (η^5-C_5R_5), R = H (Cp) or CH_3 (Cp*)] has played an important role in developing our understanding particularly because the infrared ν(C—O) bands are a useful spectroscopic tool for characterizing the reactive intermediates and monitoring the C—H activation reaction (5, 6). Photolysis results in CO loss and coordination of the alkane followed by C—H activation to form the alkyl hydride product. Elegant experiments in liquefied krypton and xenon at cryogenic temperatures demonstrated that, on the microsecond time scale, Cp*Rh(CO)Ng (Ng = Xe or Kr) was the primary photoproduct following photolysis of Cp*Rh(CO)$_2$ in either liquefied krypton or xenon. Irradiation of a mixture of alkane and *l*Kr solution resulted in formation of the noble gas complex CpRh(CO)Kr followed by the formation of the alkane complex Cp*Rh(CO)(RH), which subsequently undergoes C—H bond cleavage to give the final alkyl hydride product. Activation was observed for all alkanes studied except methane (6). In solution at room temperature, CpRh(CO)(alkane) was observed on the picosecond time scale (7) and CpRh(CO)(alkyl)H, and the only information for the rate of C—H activation was given by the slight decay on the picosecond time scale providing an estimate for the formation of the alkyl hydride, $k_{obs} = 4.0 \times 10^8$ s^{-1} ($\tau_{act} = 2.5$ ns).

The related chemistry of the Rh(Tp$^{3,5\text{-Me}}$)(CO)$_2$ [Tp$^{3,5\text{-Me}}$ = HB(3,5-dimethylpyrazolyl)$_3$] complex has been studied (8, 9), and photolysis of Rh(Tp$^{3,5\text{-Me}}$)(CO)$_2$ led to the ejection of a CO ligand and the formation of a monocarbonyl complex, which was rapidly solvated to form Rh(κ^3-Tp$^{3,5\text{-Me}}$)(CO)(RH). This species then decayed to form the more stable Rh(κ^2-Tp$^{3,5\text{-Me}}$)(CO)(RH) complex, which is able to undergo C—H activation to the final oxidative addition product, Rh(κ^3-Tp$^{3,5\text{-Me}}$)(CO)(R)H. Recent investigations into the photochemistry of the *tert*-butyl-substituted complex Rh(κ^3-Tp$^{4\text{-tBu-3,5-Me}}$)(CO)$_2$ provided additional evidence on the mechanism. The important step controlling C—H activation in this system is partial rechelation of the Tp ligand to Rh, which forms a less stable intermediate that leads to a product with a fully coordinated Tp (10).

Although there were earlier studies of C—H activation on bare metals and simple model complexes, the computational studies presented in this paper applied density functional theory (DFT) to the reaction of CpRh(CO) with CH_4 including the initial σ-complex, transition state, and methyl-hydride product (11). This work was followed shortly by complementary ab initio studies, which showed that the computed thermodynamic values for C—H activation were very sensitive to the computational method and somewhat sensitive to the basis set (12–14). Of particular

Author contributions: M.W.G. and M.B.H. designed research; O.S.J., P.P., X.-Z.S., M.T., H.W., X.Y., and S.D.Z. performed research; M.W.G. and X.-Z.S. contributed new reagents/analytic tools; M.W.G., M.B.H., O.S.J., P.P., X.-Z.S., H.W., X.Y., and S.D.Z. analyzed data; and M.W.G. and M.B.H. wrote the paper.

The authors declare no conflict of interest.

This article is a PNAS Direct Submission.

[1]To whom correspondence should be addressed. E-mail: mike.george@nottingham.ac.uk.

[2]Present address: Department of Chemistry, University of Sheffield, Brook Hill, Sheffield S3 7HF, United Kingdom.

This article contains supporting information online at www.pnas.org/lookup/suppl/doi:10.1073/pnas.1001249107/-/DCSupplemental.

relevance to this paper are the studies by Jones and co-workers on the tris(pyrazolyl)borato rhodium complexes,$Rh(Tp^{3,5\text{-}Me})(CNR)(alkyl)H$ (R = neopentyl) where the thermodynamic preference for a wide variety of hydrocarbon substrates was investigated (15). In addition to the C–H activation process, the formation of the initial alkane σ-complex and the migration of the metal along the alkane chain prior to activation play important roles in the overall reaction.

The combination of supercritical fluids and time-resolved infrared (TRIR) spectroscopy has allowed the characterization of a series of organometallic noble gas complexes at room temperature (16)—an approach that also allows the interaction of the lighter alkanes to be probed in solution at room temperature. In this paper we show that the combination of high precision fast TRIR measurements monitoring the C–H activation of alkanes by $Cp'Rh(CO)_2$ together with coupled cluster and density functional calculations yields previously undescribed insight into the factors controlling carbon-hydrogen bond activation. In particular, we report the monitoring of the activation of alkanes (n = 1–10) and demonstrate that there are significant changes in the rate of primary carbon-hydrogen activation depending solely on the length of the alkane chain.

Results and Discussion

The ns-TRIR spectra obtained following irradiation (267 nm) of $CpRh(CO)_2$ (**1**) dissolved in $scCH_4$ (4,000 psi) in the presence of CO (60 psi) are shown in Fig. 1. It is clear from the transient IR spectrum obtained 1 ns after laser flash that the parent absorptions at 1,995 and 2,056 cm^{-1} are bleached and a major new transient band is produced at 1,976 cm^{-1}. This can be readily assigned to the methane complex $CpRh(CO)(CH_4)$ (**2**) by comparison with the results obtained from previous TRIR experiments (17). Within 20 ns following laser flash, $CpRh(CO)(CH_4)$ (**2**) has decayed completely and is replaced by a new band at 2,034 cm^{-1}, which is assigned to the C–H activated alkyl hydride complex $CpRh(CO)(CH_3)H$ (**3**).

$CpRh(CO)(CH_3)H$ was already visible in the TRIR spectrum obtained 1 ns after laser flash and grows in at the same rate ($k_{obs} = 3.3(\pm0.2) \times 10^8$ s^{-1}) as $CpRh(CO)(CH_4)$ decays ($k_{obs} = 3.3(\pm0.2) \times 10^8$ s^{-1}); see Fig. 2. The lifetime of the C–H activation reaction, 3.0(±0.2) ns, is very similar to that reported (7) for the activation of the analogous pentane complex (4.0×10^8 s^{-1}). This was quite unexpected, and we have repeated the measurement of the activation of CpRh(CO)(pentane) to form CpRh(CO)(pentyl)H and found the lifetime for C–H activation of pentane to be 9.4 (±0.2) ns; see Fig. 2.

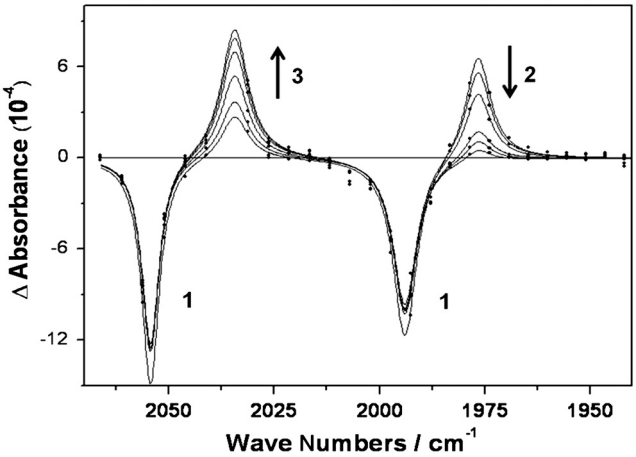

Fig. 1. Time-resolved IR spectra obtained following photolysis of $CpRh(CO)_2$ (**1**) in $scCH_4$ showing the depletion of **1** and the formation and subsequent decay of $CpRh(CO)(CH_4)$ (**2**) to form $CpRh(CO)(CH_3)H$ (**3**).

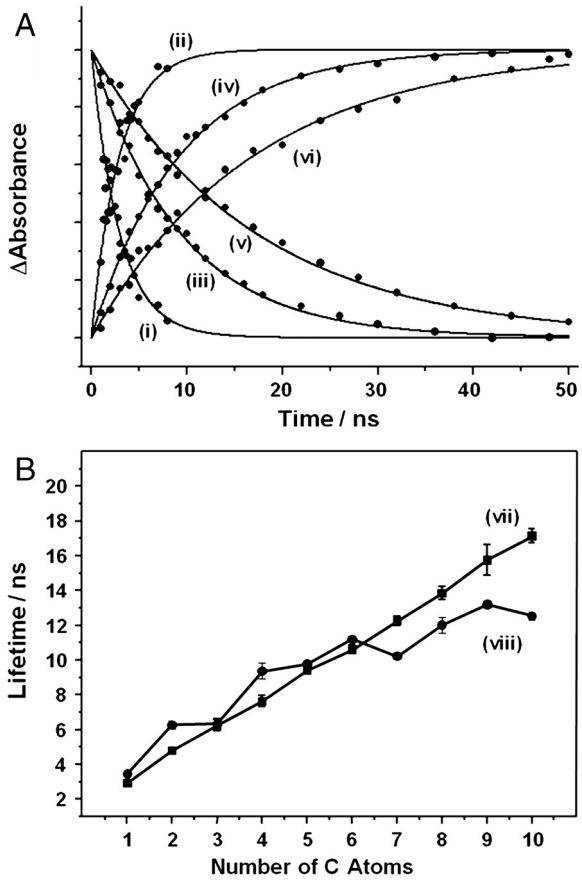

Fig. 2. (*A*) Normalized TRIR kinetic traces showing the decay of CpRh(CO)(alkane) and the formation of CpRh(CO)(alkyl)H obtained following irradiation of a solution in either $scCH_4$ [(i), (ii)], C_5H_{12} [(iii), (iv)], or $C_{10}H_{22}$ [(v), (vi)]. (*B*) A plot of the lifetimes for the C–H activation reaction for the linear alkanes as a function of C the number of carbon atoms for (vii) CpRh(CO)(alkane) and (viii) Cp*Rh(CO)(alkane).

The rate constant we have determined is clearly and significantly different from the rate measured for conversion of $CpRh(CO)(CH_4)$ to $CpRh(CO)(CH_3)H$. $CpRh(CO)(CH_3)H$ is not stable, and we have also investigated the rate of decay of $CpRh(CO)(CH_3)H$ in $scCH_4$ in the presence of CO on a much longer time scale. $CpRh(CO)(CH_3)H$ decays to regenerate the $CpRh(CO)_2$ [$k_{obs} = 3.0(\pm0.3) \times 10^3$ s^{-1}]. This rate depends linearly on the CO concentration. The rate constant for this reaction in $scCH_4$ is $k_{CO} = 7.0(\pm0.2) \times 10^3$ dm^3 mol^{-1} s^{-1}. The ability to distinguish between the rate of C–H activation in CH_4 and C_5H_{12} prompted us to investigate the rate of C–H activation for both Rh(Cp′)(CO)(alkane) (Cp′ = Cp or Cp*); see Fig. 2. The lifetime of CpRh(CO)(alkane) shows a nearly linear behavior with respect to the length of the alkane chain, and the related Cp*Rh(CO)(alkane) has a clear oscillatory behavior upon changing the alkane. However, closer inspection of the CpRh(CO)(alkane) shows that it also has an oscillatory behavior that seems partly out of phase with the rates obtained for the Cp*Rh(CO)(alkane) complexes.

The variation in rate constant can be seen from the results of plotting the residual from either a linear, CpRh(CO)(alkane), or polynomial, Cp*Rh(CO)(alkane), fit to the behavior to the C–H activation rate with alkane chain length from methane to decane (see *SI Text*). Although there is apparent oscillatory behavior for the variation in the C–H activation rate with chain length for the CpRh(CO)(alkane) system, these changes are within the experimental error of the measurements. However, the change in the C–H activation rate for the Cp*Rh(CO)(alkane)

is more marked and is greater than the errors in the rate measurement.

Computational chemistry is a very important technique for understanding the details of transition metal reactions (18) where experimental results often do not have the "resolution" to confirm details of mechanisms. Although the oxidative C—H activation by transition metal complexes has been extensively studied by computational means (19), here, higher level and more detailed calculations of the interactions of alkanes with both CpRh(CO) and Cp*Rh(CO) are made in order to understand the surprising pattern of lifetimes observed experimentally.

$$M + R{-}H \rightarrow R{-}H{\cdots}M \rightarrow R{-}M{-}H. \qquad [1]$$

As suggested by previous studies, the C—H activation proceeds in two steps (expression **1**), and it has become increasingly clear that alkane complexes, R—H···M, in which the alkanes are bound to the metal centers as "σ-complexes," without their C—H bonds being fully broken, are implicated as intermediates in the overall reaction. For these transient alkane complexes, the Rh coordination center may bind to each of the methylene (—CH_2—) and methyl (—CH_3) sites of longer alkanes (C_nH_{2n+2}, $n \geq 3$) and migrate between these sites.

The short observed lifetimes point to very low barriers for C—H activation in these Rh complexes. At the B3LYP level the CpRh(CO) enthalpic barriers are 5.4, 6.2, and 6.1 kcal mol^{-1} for CH_4, C_2H_6, and C_3H_8 (primary CH_3), respectively, whereas at the Perdew–Burke–Ernzerhof (PBE) level, these same barriers are even lower, 1.3, 1.8, and 1.7 kcal mol^{-1}. Although the differences in the barriers are similar for the two functionals, the obvious absolute discrepancy between these two functionals prompted us to perform additional calculations at the coupled cluster single and double (CCSD) level on the geometries obtained at both B3LYP and PBE levels. The "CCSD/B3LYP barriers" for CpRh(CO) are 4.7, 5.2, and 4.7 kcal mol^{-1} for CH_4, C_2H_6, and C_3H_8, respectively, whereas those for the bulky, but electron-rich, Cp*Rh(CO) complex are 4.5, 4.8, and 4.4 kcal mol^{-1} for CH_4, C_2H_6, and C_3H_8.

The relative barrier for activating different C—H bonds is also a crucial issue. Consistent with the experimental observation, for longer alkanes (C_nH_{2n+2}, $n \geq 3$), Rh complexes preferentially activate terminal or primary C—H bonds over secondary ones although the primary C-H bonds are substantially stronger than the secondary ones. For example, at CCSD//B3LYP, the C—H CpRh(CO) activation energies for C_3H_8 are 4.7 kcal mol^{-1} for CH_3 and 5.0 kcal mol^{-1} for -CH_2-, and this selectivity is even larger for the bulker Cp* system, 4.4 kcal mol^{-1} for CH_3 and 5.5 kcal mol^{-1} for CH_2. A similar trend exists for the activations in longer alkanes and barriers for CH_2 attached to —C_2H_5 are greater than those attached to —CH_3 by about 0.8 kcal mol^{-1}.

Binding to Rh occurs primarily through one C—H bond at any one instant and the rearrangement among geminal H atoms is very easy, but migrations to other CH_x groups have higher barriers. All studies to date have assumed that this migration occurs from one CH_x group to the adjoining one by 1,2-migration. For CpRh(CO)(C_3H_8) at the CCSD//PBE level, the 1,2-migration (the secondary alkane complex → the primary alkane complex for C_3H_8) requires 5.45 kcal mol^{-1} of activation energy, whereas the 1,3-migration (migration between the two terminal CH_3 groups for C_3H_8) is easier, needing only 4.25 kcal mol^{-1} of activation energy. The migration barriers by Cp*Rh(CO) are much lower than those by CpRh(CO), 4.39 kcal mol^{-1} for 1,2-migration and 3.39 kcal mol^{-1} for 1,3-migration for C_3H_8. In terms of the overall thermodynamics of binding both Cp- and Cp*Rh(CO) bind primary CH groups more strongly than secondary ones, and the binding energy in CpRh(CO) is greater than that of Cp*Rh (CO). This difference and the difference between this pattern and that predicted previously for $W(CO)_5$ binding (20) appears to be dominated by steric differences.

For linear alkanes experimental *gauche-trans* energy differences were reported ranging from approximately 0.5 to 1.0 kcal mol^{-1} (21–23) in the gas phase and are in the range of 0.5–0.6 kcal mol^{-1} in the liquid (22). An electron diffraction study of the alkanes butane through heptane revealed that the gas-phase conformations often contain *gauche* dihedral angles (24), and earlier molecular dynamics studies predicted that *gauche* population should be enhanced upon transfer from the gas phase to the liquid (25). Hence, for larger alkanes ($n > 3$) both the *gauche* and *trans* conformations are present in the liquid state. Furthermore, in the *gauche* conformation, 1,4-migrations are also possible. For end-to-end migration in *gauche* butane, the activation energy for the 1,4-migration is about 0.5 kcal mol^{-1} higher than that for the 1,3-migration, but about 1.0 kcal mol^{-1} less than that for the 1,2-migration. We also compared the C—H activation barriers for the three terminal hydrogens of both *trans* and *gauche* linear butanes (see Fig. 3). Generally, the average enthalphic barriers at CH_3 were slightly larger for the *gauche* isomers for both Cp and Cp*. However, the free energy barriers were significantly larger for the *gauche* isomer in the Cp* case.

Although only shorter hydrocarbons ($n \leq 3$) were studied at the CCSD level, we examined long alkane chains at the PBE level. Fig. 3*C* summarizes the C—H activation enthalpies vs. number of carbon atoms for the *all-trans* linear alkanes ($n = 1$ to 10) by CpRh(CO) and Cp*Rh(CO). Generally, the C—H activation

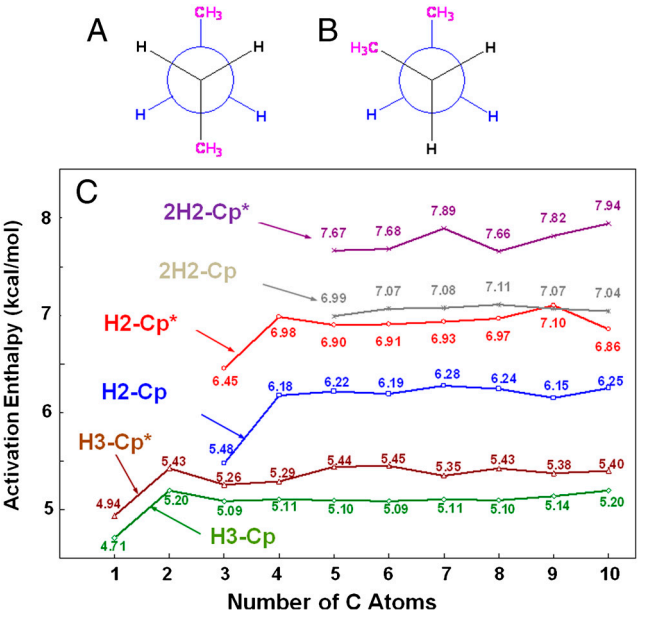

Fig. 3. Schematic representation of (*A*) *trans-n*-butane and (*B*) *gauche-n*-butane. The different terminal C—H bonds have different activation energies because of the different orientation of the alkane chain with respect to CpRh(CO). For CpRh(CO)(alkane) the average difference between *A* and *B* is 0.71 kcal mol^{-1}, whereas for Cp*Rh(CO)(alkane) the average difference is 1.93 kcal mol^{-1}. (*C*) Calculated C—H activation barriers for the primary ($C^*H_3CH_2CH_2$—) C—H bonds activation enthalpies (in kcal mol^{-1}) vs. number of carbon atoms for the linear alkanes ($n = 1$ to 10) by CpRh(CO) (**H3-Cp**; green curve) and by Cp*Rh(CO) (**H3-Cp***; brown curve) and the secondary C—H activation enthalpies (in kcal mol^{-1}) vs. number of carbon atoms for the *n*-alkanes propane through decane by CpRh(CO) (**H2-Cp**; blue curve for $CH_3C^*H_2CH_2$— and **2H2-Cp**; gray curve for $CH_3CH_2C^*H_2$—) and by Cp*Rh (CO) (**H2-Cp***; red curve for $CH_3C^*H_2CH_2$— and **2H2-Cp***; purple curve for $CH_3CH_2C^*H_2$—). All data were calculated at the PBE level and offset upward by 3.43 kcal mol^{-1} to obtain the approximate CCSD values. The offset value of 3.43 kcal mol^{-1} is the activation enthalpy difference between the PBE calculation and the CCSD//PBE calculation for methane's C—H activation by CpRh(CO).

enthalpic curves become relatively linear after propane for the $-CH_3$ activations and after butane for the $-CH_2-$ activations. The relative migration activation enthalpies vs. number of carbons for the linear alkanes ($n = 3$ to 6) is summarized in *SI Text*. From the calculated results, we can see that CpRh(CO) C–H activation energies are lower than the Cp*Rh(CO) ones, whereas both migrations (1,2- and 1,3-) are easier in the Cp*Rh(CO) system than in the CpRh(CO) system. The 1,3-migrations are faster than the 1,2-migrations because the two C–H bonds involved are much better aligned to bond well with the metal in the transition state. Secondary C–H activation barriers are much larger than both the primary C–H activation and the two migrations. Hence, C–H activation at $-CH_2-$ groups is very unlikely during the reaction with alkanes having $-CH_3$ groups. The σ-complexes formed by $-CH_2-$ groups following photolysis will migrate to terminal $-CH_3$ sites before the C–H activation takes place.

Kinetics Simulations

By using standard transition state theory with a transmission coefficient of 1.0 and the observed lifetime ($1/k$) of methane in the CpRh(CO) system (~3 ns), the free energy barrier for the C–H bond activation is calculated as 5.8 kcal mol^{-1}, which is close to our calculated (CCSD//PBE) free energy value of 6.0 kcal mol^{-1}. The lifetimes of such fast reactions are very sensitive to $\Delta G^{\ddagger}$, as an increase in the free energy barrier of 0.1 kcal mol^{-1} will bring almost 0.6-ns change in lifetime. Thus, if we want to simulate the observed lifetimes (±0.2 ns) using the calculated free energy barriers, the error of these calculations must be less than 0.02 kcal mol^{-1}. Unfortunately, this accuracy is unreachable for molecular systems containing a heavy metal atom with current theoretical and computational methods. Therefore, the calculations can be only a guide to the most important steps and the most important energy changes. The actual simulations of the experimental results will be empirical, but strongly based on computed trends and using the fewest parameters consistent with the computational and experimental results.

1. Summary of Principles Obtained from Calculations. The basic principles summarized below for the chemical kinetics simulations are based on the computed values displayed in Fig. 3 and *SI Text*.

I. For the C-H activations: (*i*) The activation energy of a C–H bond increases significantly when one of the spectator H atoms on a CH_x group being activated is replaced with a $-CH_3$ group. (*ii*) With longer alkanes, the internal $-CH_2-$ groups have higher activation energy than those attached to $-CH_3$. (*iii*) CpRh(CO) activates the C–H bonds of alkanes more easily than Cp*Rh(CO). (*iv*) Ethane has a higher C–H bond activation barrier than methane. (*v*) The C–H activation barriers at $-CH_3$ in ethane and propane are similar in CpRh(CO) but have somewhat larger differences in Cp*Rh(CO). (*vi*) Propane and longer alkanes have constant C–H bond activation barriers at their $-CH_3$ groups. (*vii*) Differences in C–H activation barriers between $-CH_3$ groups near the *gauche* turn and those farther away are larger for Cp*Rh(CO) than those for CpRh(CO) because of the crowded structure of Cp* (Fig. 3).

II. For the migrations between CH_x groups: (*i*) In the CpRh(CO) system, barriers for 1,2-migrations of alkanes are about constant and similar in magnitude to the C–H activations of $-CH_3$. (*ii*) Barriers for 1,3-migrations of alkanes are smaller than those for 1,2-migrations and decrease with increasing chain length in the CpRh(CO) system. (*iii*) Both 1,2- and 1,3-migrations have lower barriers in the Cp*Rh(CO) system because of its stronger steric effect. (*iv*) Generally, the 1,4-migration barriers are larger than 1,3-migration barriers and the differences are smaller for Cp*Rh(CO). Furthermore, because the barriers for $-CH_3$ activation near a *gauche* turn are higher for Cp*Rh(CO), the 1,4-migrations will play a larger role in the activation of Cp*Rh(CO) systems and were included in these simulations.

2. Reaction Kinetics Simulations Based on Above Principles The qualitative principles from the quantum chemical calculations discussed above form the basis for the following simulations: To determine some of the key factors in the lifetimes of alkanes in their reactions with CpRh(CO) and Cp*Rh(CO), we tested several simulations. First of all, the reactions were simulated without migration between different carbon atom positions to determine the effect of different C–H bond activation barriers at the $-CH_2-$ positions. The initial concentrations of Rh–alkane complexes were based on the statistical distribution of the numbers of C–H bonds in each alkane. The C–H activation barriers (free energy) of CH_4 and $-CH_3$ were set as 5.8 and 6.1 kcal mol^{-1} (close to the DFT calculated results and simulated from experimental lifetimes of methane and ethane). Variable $-CH_2-$ activation barriers resulting in the simulated lifetimes of alkanes are shown in the *SI Text*, where the lifetimes shorten quickly with decreasing the $-CH_2-$ activation barriers. The simulations with $-CH_2-$ activation barriers of 7.0 and 6.8 kcal mol^{-1} bracket the observed lifetimes. However, all of these lifetime trends with different $-CH_2-$ activation barriers are smooth and do not have the weak but observable step pattern obtained in experimental measurements. Furthermore, the $-CH_2-$ barrier (6.8 kcal mol^{-1}) that brings the simulated lifetime for C_4H_{10} into agreement with the experimental lifetime is only 0.7 kcal mol^{-1} larger than the $-CH_3$ barriers, although the calculations would suggest a difference close to 1.1 kcal mol^{-1}. Overall lifetimes are predicted to be too long when one applies the average calculated difference between $-CH_2-$ and $-CH_3$ barriers. Therefore, we need to consider additional aspects in the kinetics simulations, such as the migrations between different CH_x groups bonding to the Rh atom.

The results when different 1,2-migration barriers are introduced into simulations with fixed C–H activation free energy barriers for CH_4, $-CH_3$, and $-CH_2-$ of 5.8, 6.1, and 7.2 kcal mol^{-1}, respectively, are also displayed in the *SI Text*. The smaller 1,2-migration barriers reduce the simulated lifetimes of alkanes in these reactions. With 1,2-migration barriers of 6.2 kcal mol^{-1}, the simulated lifetimes are very close to the experimental values of alkanes with CpRh(CO). Again, however, the lifetimes are almost linear with the increase of the size of alkanes and do not reproduce the weak observed step pattern. Furthermore, according to the DFT calculations, 1,3-migrations are faster than 1,2-migrations and, thus, must also be introduced in the simulation.

The simulated lifetimes of alkanes with constant barriers for C–H activation of CH_4, $-CH_3$, and $-CH_2-$ (5.8, 6.1, and 7.2 kcal mol^{-1}) and 1,2-migration (7.0 kcal mol^{-1}) but different barriers for 1,3-migrations have also been investigated (*SI Text*). The plots of reaction lifetimes vs. numbers of C atoms are, of course, linear when 1,3-migrations have the same barriers as the 1,2-migrations. However, when the 1,3-migration barrier is decreased to 6.0 kcal mol^{-1}, the simulated lifetimes of alkanes begin to display an obvious but weak step pattern that matches extremely well with the experimental lifetimes of alkanes in their reactions with Cp*Rh(CO). The barriers of these 1,3-migrations are actually slightly lower than the C–H bond activation barrier. This is consistent with the quantum chemical calculations. This step pattern arises from alkanes with even carbon numbers, which due to the low barrier 1,3-migrations can move CpRh(CO) to one of the two $-CH_3$ ends without ever needing a higher barrier 1, 2-migration. However, for alkanes with an odd number of carbon atoms, migrations from some $-CH_2-$ groups will require the higher barrier of 1,2-migrations to reach either of the terminal $-CH_3$ groups. Therefore, as shown in *SI Text*, alkanes with an even number of C atoms such as 4 and 6 appear to have slightly shorter lifetimes in general agreement with the experimental

results. This step pattern becomes stronger with the decrease of the 1,3-migration barrier.

Although the simulations with the relative reaction barriers of 1,3-migration < $-CH_3$ activation < 1,2-migration < $-CH_2$ activation exactly reproduce the lifetimes of alkanes reacting with CpRh(CO), no variations of these parameters alone can explain the observed lifetime pattern of alkanes reacting with Cp*Rh(CO). The lifetimes of ethane and butane in the Cp*Rh(CO) system are about 2 ns longer than those in the CpRh(CO) system. The 1,3-migration cannot explain the longer lifetimes of butane and similar lifetime of pentane because the lower 1,3-migration barriers can lead only to a reverse pattern with shorter lifetime of butane and longer lifetime of pentane. Higher 1,3-migration barriers will lead only back to linear behavior. The calculations suggest that for the Cp*Rh(CO) system the C–H activation barriers are higher, whereas the migration barriers are lower than those in the CpRh(CO) system. In addition, because the Cp* structure is sterically more crowded, the Cp* reaction is more sensitive to the conformation of alkanes. For example, near a *gauche* turn in butane and longer alkanes, the 1,3-migration and C–H activation of $-CH_3$ are slower, but a *gauche* conformation leads to faster 1,4-migrations in pentane and longer alkanes. Furthermore, in the Cp*Rh(CO) system, the 1,2-, 1,3-, and 1,4-migration barriers become lower with increasing chain length.

The final simulations for both Cp and Cp* systems are shown in Fig. 4. In particular, Cp*Rh(CO)(butane) is longer-lived because 33% of it is in the *gauche* conformation, which activates more slowly, whereas Cp*Rh(CO)(pentane) is shorter-lived because faster migrations can move the σ-complexes to the end without the *gauche* turn. As the chains get longer, there is a higher probability of *gauche* turns, which shortens the lifetimes ($n = 7$). Here and in longer alkanes, conformations with multiple *gauche* turns further complicate the analysis such that simple explanations from static calculations alone cannot be made. When all of these additional effects are introduced into our simulations, a lifetime pattern of alkanes with Cp*Rh(CO) very close to the experimental results is obtained. Heptane has a somewhat larger error as we have simulated it using only three conformations, although in reality it has many more including several with two *gauche* turns.

Concluding Remarks

Surprisingly, for the CpRh(CO)(alkane) system there is an approximately linear relationship between lifetime and alkane chain length that is unexpected because major differences between primary and secondary alkanes should have a dramatic effect on changing from methane and ethane to heavier alkanes and eventual asymptotic behavior with long chain lengths. Our understanding of the delicate balance in the factors controlling this fundamental reaction came from studying the related Cp*Rh(CO)(alkane) system where an oscillating and asymptotic behavior was observed. Indeed close inspection of the CpRh(CO)(alkane) system revealed a complementary oscillatory behavior albeit barely observable in this unique experimental dataset.

These data have been understood by using theoretical calculations. As we have previously shown, the barrier for oxidative cleavage of the C–H bond by transition metal complexes is sensitive to the functional and somewhat sensitive to the basis set. Because of the sensitivity required to disentangle these experimental results, we have carried out CCSD calculations. The CCSD calculations were combined with the DFT trends to develop kinetic simulations that reproduced the experimentally observed rates of oxidative cleavage and chain migration and led to the elucidation of the mechanism of C–H activation. Our results clearly show that an understanding of the barriers to primary and secondary alkane activation, the rates of 1,2- and 1,3-migrations of the coordination center along the chain, and the importance of the conformation (*trans* vs. *gauche*) of the coordinated alkane is required in order to predict the behavior of these fundamental reactions. The observed variation in lifetimes arises from a subtle competition between activation and migration.

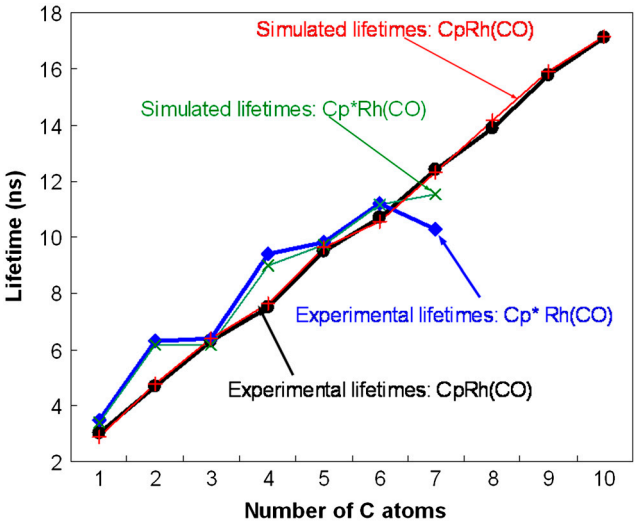

Fig. 4. Final simulated and experimental lifetimes are compared.

Materials and Methods

1. Quantum Calculation Details. All calculations were performed using the Gaussian 03 suite of ab initio programs for both CCSD and DFT computations. (26) The geometric structures of all species were optimized in the gas phase at the PBE level. For the shorter hydrocarbons ($n \leq 3$), the full optimizations were carried out at the B3LYP level, and the single-point calculations with the basis set superposition error (BSSE) corrections were carried out at the CCSD level on the structures obtained at both B3LYP and PBE levels. Stuttgart/Dresden RSC 1997 (SDD) effective core potential and basis set (SDD) was used for the Rh atom, and the cc-pVDZ basis set was applied for all other atoms. Calculating the harmonic vibrational frequencies and noting the number of imaginary frequencies confirmed the nature of all intermediates (no imaginary frequency) and transition state structures (only one imaginary frequency). The latter were also confirmed to connect reactants and products by intrinsic reaction coordinate calculations. The gas-phase free energies, G, were calculated at $T = 298.15$ K within the harmonic potential approximation at optimized structures. No solvent effects were taken into account as these reactions involve uncharged reactants, transition states, and products in weakly coordinating liquid hydrocarbons.

2. Experimental Details. $CpRh(CO)_2$ was prepared in adaptation to a published procedure (27). $Cp^*Rh(CO)_2$ was purchased from Strem Chemicals, Inc. The gases argon (99.994%) and methane (grade 4.5) were purchased from Air Products; CO (>99%), ethane, propane (98%+), and butane (99.5%) were purchased from Aldrich and used as received. The liquid alkanes were heated to reflux over CaH_2 for several hours. The TRIR experiments were performed at the Picosecond Infrared Absorption and Transient Excitation facility at the Rutherford Appleton Laboratory, which also has been described in detail elsewhere (28).

ACKNOWLEDGMENTS. We acknowledge Professors A. W. Parker and P. Matousek for helpful discussions. We thank the Engineering and Physical Sciences Research Council and the European Union (P.P. FP6- 502440) for financial support. M.W.G. is particularly grateful to the Royal Society for the award of a Wolfson Merit Award. The theoretical calculation and simulation work were supported by grants from National Science Foundation (CHE-0910552, CHE-0518074, CHE-0541587, and DMS-0216275), the Welch Foundation (A0648), and the Serbian Ministry of Science (142037).

1. Derouane EG, Haber J, Lemos F, Ribeiro FR, Guimet M (1998) *Catalytic Activation and Functionalisation of Light Alkanes. Advances and Challenges* (Kluwer, Dordrecht, The Netherlands).

2. Arndtsen BA, Bergman RG, Mobley TA, Peterson TH (1995) Selective intermolecular carbon-hydrogen bond activation by synthetic metal complexes in homogeneous solution. *Acc Chem Res* 28:154–162.

3. Janowicz AH, Bergman RG (1982) Carbon-hydrogen activation in completely saturated hydrocarbons: Direct observation of $M + R{-}H \rightarrow M(R)(H)$. *J Am Chem Soc* 104:352–354.
4. Hoyano JK, Graham WAG (1982) Oxidative addition of the carbon-hydrogen bonds of neopentane and cyclohexane to a photochemically generated iridium(I) complex. *J Am Chem Soc* 104:3723–3725.
5. Belt ST, Grevels F-W, Klotzbücher WE, McCamley A, Perutz RN (1989) Intermediates in the time-resolved and matrix photochemistry of (η^5-cyclopentadienyl)rhodium complexes: Roles of alkane activation and rhodium-rhodium bond formation. *J Am Chem Soc* 111:8373–8382 and references therein.
6. McNamara BK, Yeston JS, Bergman RG, Moore CB (1999) The effect of alkane structure on rates of photoinduced C—H bond activation by $Cp^*Rh(CO)_2$ in liquid rare gas media: An infrared flash kinetics study. *J Am Chem Soc* 121:6437–6443 and references therein.
7. Asbury JB, Ghosh HN, Yeston JS, Bergman RG, Lian TQ (1998) Sub-picosecond IR study of the reactive intermediate in an alkane C—H bond activation reaction by $CpRh(CO)_2$. *Organometallics* 17:3417–3419.
8. Bromberg SE, et al. (1997) The mechanism of a C-H bond activation reaction in room-temperature alkane solution. *Science* 278:260–263.
9. Zarić S, Hall MB (1998) Prediction of the reactive intermediates in alkane activation by tris-pyrazolylborate rhodium carbonyl. *J Phys Chem A* 102:1963–1964.
10. Blake AJ, et al. (2008) Probing the mechanism of carbon-hydrogen bond activation by photochemically generated hydridotris(pyrazolyl)borato carbonyl rhodium complexes: New experimental and theoretical investigations. *Organometallics* 27:189–201.
11. Ziegler T, Tschinke V, Fan L, Becke AD (1989) Theoretical study on the electronic and molecular structures of $(C_5H_5)M(L)$ (M = rhodium, iridium; L = carbonyl, phosphine) and $M(CO)_4$ (M = ruthenium, osmium) and their ability to activate the carbon-hydrogen bond in methane. *J Am Chem Soc* 111:9177–9185.
12. Song J, Hall MB (1993) Theoretical studies of inorganic and organometallic reaction mechanisms 6: Methane activation on transient cyclopentadienylcarbonylrhodium. *Organometallics* 12:3118–3126.
13. Siegbahn PEM (1996) Comparison of the C-H activation of methane by M(C5H5)(CO) for M = cobalt, rhodium, and iridium. *J Am Chem Soc* 118:1487–1496.
14. Couty M, Bayse CA, Jimenez-Catano R, Hall MB (1996) Controversial exothermicity of the oxidative addition of methane to (cyclopentadienyl)rhodium carbonyl. *J Phys Chem* 100:13976–13978.
15. Clot E, Eisenstein O, Jones WD (2007) Coordination chemistry of saturated molecules special feature: Structural and dynamic properties of propane coordinated to TpRh (CNR) from a confrontation between theory and experiment. *Proc Natl Acad Sci USA* 104:6939–6944 and references therein.
16. Kuimova MK, et al. (2003) Using picosecond and nanosecond time-resolved infrared spectroscopy for the investigation of excited states and reaction intermediates of inorganic systems. *Dalton Trans* 3996–4006.
17. Weiller BH, Wasserman EP, Bergman RG, Moore CB, Pimentel GC (1989) Time-resolved IR spectroscopy in liquid rare gases: Direct rate measurement of an intermolecular alkane carbon-hydrogen oxidative addition reaction. *J Am Chem Soc* 111:8288–8290.
18. Niu S, Hall MB (2000) Theoretical studies on reactions of transition-metal complexes. *Chem Rev* 100:353–406 and references therein.
19. Balcells D, Clot E, Eisenstein O (2010) C-H bond activation in transition metal species from a computational perspective. *Chem Rev* 110:749–823 and references therein.
20. Zarić S, Hall MB (1997) Ab initio calculations of the geometries and bonding energies of alkane and fluoroalkane complexes with tungsten pentacarbonyl. *J Phys Chem A* 101:4646–4652.
21. Jorgensen WL (1983) Theoretical studies of medium effects on conformational equilibria. *J Phys Chem* 87:5304–5314.
22. Thomas LL, Christakis TJ, Jorgensen WL (2006) Conformation of alkanes in the gas phase and pure liquids. *J Phys Chem B* 110:21198–21204.
23. Tsuzuki S, et al. (1991) Investigation of intramolecular interactions in n-alkanes. Cooperative energy increments associated with GG and GTG′ [G = gauche, T = trans] sequences. *J Am Chem Soc* 113:4665–4671.
24. Bartell LS, Kohl DA (1963) Structure and rotational isomerization of free hydrocarbon chains. *J Chem Phys* 39:3097–3105.
25. Pratt LR, Hsu CS, Chandler D (1978) Statistical mechanics of small chain molecules in liquids. I. Effects of liquid packing on conformational structures. *J Chem Phys* 68:4202–4212.
26. Frisch MJ, et al. (2004) *Gaussian 03, Revision D.02, Suite of Programs for Ab Initio Calculation* (Gaussian, Inc, Wallingford, CT).
27. Bittler K, Fischer EO (1961) Aromatic complexes of metals. XLII. Cyclopentadienyl-rhodium-dicarbonyl. *Z Naturforsch B* 16:225.
28. Towrie M, et al. (2003) Development of a broadband picosecond infrared spectrometer and its incorporation into an existing ultrafast time-resolved resonance Raman, UV/visible, and fluorescence spectroscopic apparatus. *Appl Spectrosc* 57:367–380.